WATER RESOURCES RESEARCH, VOL. 32, NO. 11, PAGES 3385–3389, NOVEMBER 1996

Analytical integration of the kinematic equation for runoff on a plane under constant rainfall rate and Smith and Parlange infiltration

J. V. Giráldez
Departmento de Agronomía, Universidad de Córdoba, Córdoba, Spain

D. A. Woolhiser
Department of Civil Engineering, Colorado State University, Fort Collins

Abstract. An analytical solution to the kinematic wave approximation of the Saint-Venant equations describing surface water flow with infiltration is presented. Adopting the Smith and Parlange formulation for the ponding time and the postponding infiltration rate, a change of variable among time and infiltration rate allow the analytical integration of the characteristic equations when the flow rate is expressed as the second power of the water depth. In the case of any other real exponent a simple numerical integration method may be used for the computation of the characteristic curves. An illustration is made to compare the solutions for different values of the exponent, as well as to assess the accuracy of some numerical schemes.

Introduction

Surface runoff flow is often described by the kinematic wave approximation of the Saint-Venant equations. In this way, water flow is known after integration of both the continuity or mass conservation equation and the dynamic or momentum conservation equation. The continuity equation states that the combination of the time variation of water depth h, at any point, and the change of flow rate q, with distance x, equals the excess of rainfall,

$$\frac{\partial h}{\partial t} + \frac{\partial q}{\partial x} = r - f \tag{1}$$

where t stands for time and r and f for rainfall and infiltration rates, respectively. One simplification of the dynamic equation is the relation for uniform flow between flow rate and water depth,

$$q = \alpha h^m \tag{2}$$

where α is a coefficient expressing surface conditions for the flow and m is an exponent. Common initial and boundary conditions of surface flow are null water depth

$$h(0, t) = h(x, 0) = 0 \tag{3}$$

These equations can be solved by the method of characteristics [*Courant and Hilbert*, 1962, Section II.2], which converts the partial differential equations to a pair of ordinary differential equations, expressing the absolute time variation of water depth,

$$dh/dt = r - f \tag{4}$$

along the characteristic curve,

$$dx/dt = \alpha m h^{m-1} \tag{5}$$

or any other combination of them.

Paper number 96WR02106.
0043-1397/96/96WR-02106$09.00

These equations have known analytical solutions for certain cases of rainfall and infiltration rates in simple geometrical configurations. For a plane and uniform rain of constant rate *Henderson and Wooding* [1964] and *Wooding* [1965] presented a solution, extended later by *Sherman and Singh* [1976] and *Sherman* [1978] to the case of space dependency of the α parameter. *Hjelmfelt* [1978] introduced a time variable infiltration rate adapting the curve number method of the Soil Conservation Service. *Cundy and Tento* [1985] and *Luce and Cundy* [1992] derived an analytical solution for these equations when the infiltration rate followed the Philip two-term formula. Nevertheless, neither of the above mentioned equations was developed for the infiltration of water in the soil under rainfall or flux conditions. One of the most versatile expressions for the description of this process is the *Smith and Parlange* [1978] equations, extensively used in hydrology models, for example, KINEROS [*Woolhiser et al.*, 1990], but numerically integrated. The purpose of this report is to illustrate the development of an analytical solution to the kinematic wave equations using the *Smith and Parlange* [1978] method to compute the infiltration rate.

Development of Water Depth and Flow Rates in the Different Integration Domains

In the same plane geometry of other authors like *Wooding* [1965], the characteristic curves may be grouped in several regions or domains depending on their origin: the distance axis at the time of ponding for the first domain, the part of the time axis from t_p up to the rain duration for the second domain, and the rest of the $x - t$ plane for the third domain, all of them representing distinct physical conditions. The integration of the kinematic equations will be presented in these three domains.

Domain 1: Characteristics Originating at $(0 < x < L, t = t_p)$

For any rainfall rate greater than the saturated hydraulic conductivity of the soil K_s, starting at time $t = 0$, runoff water

Table 1. Soil, Slope, and Rainfall Parameters

	Soil		Slope		Rainfall	
Case	K_s, mm h^{-1}	$S^2/2$, mm^2 h^{-1}	α, s^{-1}	L, m	r, mm h^{-1}	t_r, min
A	10	355.	0.25	100	20	399.
B	1	76.3	0.25	100	20	258.
C	1	76.3	28.3	5	400	1.37
D	10	355.	28.3	5	20	285.
E	10	355.	0.707	100	400	42.5

begins to flow at ponding time t_p, computed as [*Smith and Parlange*, 1978]

$$t_p = \frac{S^2}{2rK_s} \ln\left(\frac{r}{r - K_s}\right) \tag{6}$$

with S as the sorptivity. If the rain ends at a large enough time, the integration of (4) is

$$\int_0^h dh = \int_{t_p}^t (r - f)\, dt \tag{7}$$

The infiltration rate f, according to *Smith and Parlange* [1978], is implicitly given by

$$t - t_p = \frac{S^2/2}{K_s^2}\left[\ln\left(\frac{r - K_s}{r}\frac{f}{f - K_s}\right) - \frac{K_s}{f} + \frac{K_s}{r}\right] \tag{8}$$

To perform the integration on the right-hand side of (7), it is convenient to change the independent variable from time to infiltration rate, leading to

$$h = \int_{t_p}^t (r - f)\, dt = (r - f)(t - t_p) - \int_f^r (t - t_p)\, df \tag{9}$$

with the solution as

$$h = \frac{S^2/2}{K_s^2}\left\{(r - K_s)\ln\left(\frac{r - K_s}{r}\frac{f}{f - K_s}\right) - (r - f)\frac{K_s}{f}\right\} \tag{10}$$

The equation for the characteristic curve is now

$$\int_{x_o}^x dx = m\alpha \int_{t_p}^t h^{m-1}\, dt = m\alpha \int_0^h \frac{h^{m-1}\, dh}{r - f}$$

$$= -m\alpha \frac{S^2}{2} \int_f^r \frac{h^{m-1}\, df}{f^2(f - K_s)} \tag{11}$$

The integral on the right-hand side of (11) has an analytical solution for the case $m = 2$ as suggested by *Wooding* [1965] for some cases of overland flow.

$$x - x_o = 2\alpha\left(\frac{S^2/2}{K_s}\right)^2 \left\{\frac{r^2 - f^2}{2rf^2} + \frac{r - K_s}{K_s}\right.$$

$$\cdot\left[-\frac{1}{f} + \frac{1}{2K_s}\ln\left(\frac{r - K_s}{r}\frac{f}{f - K_s}\right)\right]$$

$$\left.\cdot \ln\left(\frac{r - K_s}{r}\frac{f}{f - K_s}\right)\right\} \tag{12}$$

It should be noted that $m = 2$ is not an unrealistic value for overland flow. Theory, reinforced by experiment, predicts that overland flow on a smooth, planar surface begins as laminar flow ($m = 3$) over part of the plane, but the zone near the upstream boundary will remain laminar. During the recession there will be a transition from turbulent to laminar flow. As a practical matter, small surface irregularities will often lead to mixed laminar and turbulent conditions over part of the surface, so an exponent between 3 and 5/3 may be more appropriate than one of 5/3. For example, *Wooding* [1965] adopted the value $m = 2$ for overland flow based on experimental data on several types of surfaces analyzed by *Henderson and Wooding* [1964, Table 1]. It is beyond the scope of this technical note to discuss resistance equations for overland flow in detail; however, a good discussion can be found in the work by *Singh* [1966]. If m assumes any other real value, the explicit form of h in (10) allows a straightforward solution with a simple numerical integration.

Domain 2: Characteristics Originating at ($x = 0, t_p < t < t_r$)

The characteristic curves in the second domain emanate from the time axis at time $t_o > t_p$. The water depth changes in time as indicated by

$$h = \int_{t_o}^t (r - f)\, dt = (r - f)(t - t_o) - \int_f^{f_o} (t - t_o)\, df \tag{13}$$

where f_o is the infiltration rate at the time t_o. Consequently,

$$h = \frac{S^2/2}{K_s^2}\left[(r - K_s)\ln\left(\frac{f_o - K_s}{f_o}\frac{f}{f - K_s}\right) - rK_s\left(\frac{1}{f} - \frac{1}{f_o}\right)\right] \tag{14}$$

The characteristic curves are now

$$\int_0^x dx = m\alpha \int_{t_o}^t h^{m-1}\, dt \tag{15}$$

as before for the special case of $m = 2$, the complete equation is

$$x = -2\alpha\left(\frac{S^2/2}{K_s}\right)^2\left\{\frac{r - f_o}{f_o}\left(\frac{1}{f} - \frac{1}{f_o}\right) - \frac{r}{2}\left(\frac{1}{f^2} - \frac{1}{f_o^2}\right)\right.$$

$$+\left[\left(\frac{r - K_s}{fK_s} - \frac{r - f_o}{f_oK_s}\right) - \frac{r - K_s}{2K_s^2}\right.$$

$$\left.\left.\cdot \ln\left(\frac{f_o - K_s}{f_o}\frac{f}{f - K_s}\right)\right]\ln\left(\frac{f_o - K}{f_o}\frac{f}{f - K}\right)\right\} \tag{16}$$

Domain 3: From the End of the Rain Until the Exhaustion of Water on the Surface

After rain ceases, water excess is negative, being equal to the infiltration rate as long as there is some water depth on the surface,

$$dh/dt = -f, \tag{17}$$

which is integrated as

$$h - h_* = \int_{t_r}^t -f\, dt = -f(t - t_r) - \int_f^{f_r} (t - t_o)\, df \tag{18}$$

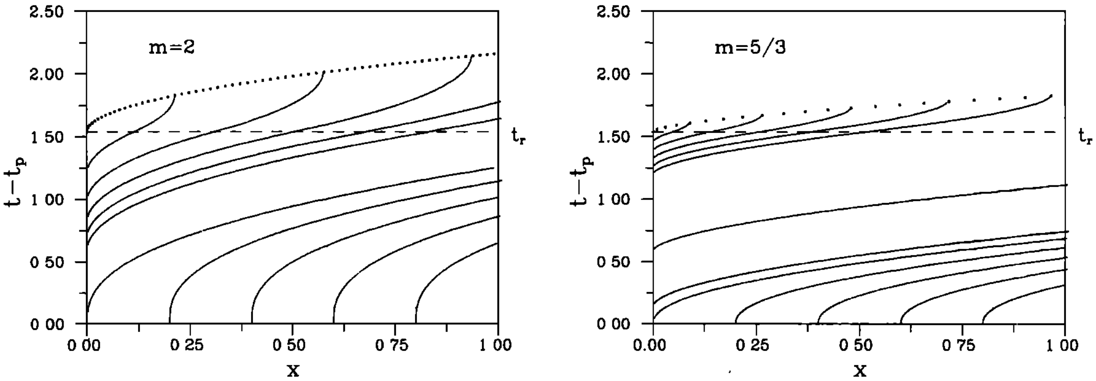

Figure 1. Characteristic curves for case A, computed by (a) the analytical solution, $m = 2$ and (b) the semianalytical solution with numerical integration, $m = 5/3$. The horizontal dashed line is the isochrone for the end of the rain. The top dotted line is the zero water depth line. Distance is normalized with respect to plane length L, and time is normalized with respect to saturated hydraulic conductivity and sorptivity $S^2/(2K_s^2)$.

where f_r is the infiltration rate at the end of the rainfall t_r and h_* is the water depth at any position x_* in the limiting characteristic for time t_r. The integration yields

$$h - h_* = -\frac{S^2/2}{K_s} \ln\left(\frac{f}{f-K_s}\frac{f_r-K_s}{f_r}\right) \tag{19}$$

The flow ends at any point when water depth goes to zero, which happens at the time the infiltration rate is f_{zw},

$$f_{zw} = K_s\left[1 - \frac{f_r - K_s}{f_r}\exp\left(-\frac{h_* K_s}{S^2/2}\right)\right]^{-1} \tag{20}$$

The characteristic curves start from the position of the previous domain, x_*, at time t_r, with water depth h_*. Proceeding as before,

$$\int_{x_*}^{x} dx = m\alpha \int_{t_r}^{t} h^{m-1}\,dt = -m\alpha \frac{S^2}{2}\int_{f}^{f_r} \frac{h^{m-1}\,df}{f^2(f-K_s)} \tag{21}$$

For the case of $m = 2$ the solution is

$$x - x_* = 2\alpha\left(\frac{S^2/2}{K_s^2}\right)\left\{\left(h_* - \frac{S^2/2}{K_s}\right)\left(\frac{K_s}{f} - \frac{K_s}{f_r}\right) + \left[\frac{S^2/2}{K_s}\left(\frac{f-K_s}{f} + \frac{1}{2}\ln\left[\frac{f}{f-K_s}\frac{f_r-K_s}{f_r}\right]\right) - h_*\right] \cdot \ln\left(\frac{f}{f-K_s}\frac{f_r-K_s}{f_r}\right)\right\} \tag{22}$$

Therefore the position x_{zw} of the vanishing water depth is given by

$$x_{zw} = x_* + 2\alpha\left(\frac{S^2}{2}\right)^2 K_s\left\{\frac{K_s}{f_r} - \frac{K_s}{f_{zw}} + \left[\left(1 - \frac{K_s}{f_r}\right) - \frac{1}{2}\ln\frac{f_{zw}}{f_{zw}-K_s}\frac{f_r-K_s}{f_r}\right]\ln\frac{f_{zw}}{f_{zw}-K_s}\frac{f_r-K_s}{f_r}\right\} \tag{23}$$

Applications

To illustrate the convenience of the characteristics and analytical solution, hydrographs have been calculated for the set of combinations of soil, slope, and rainfall conditions summarized in Table 1. These cases represent combinations of high and low rainfall excess rates with rapidly and slowly responding runoff planes. Some of the characteristic curves for the inte-

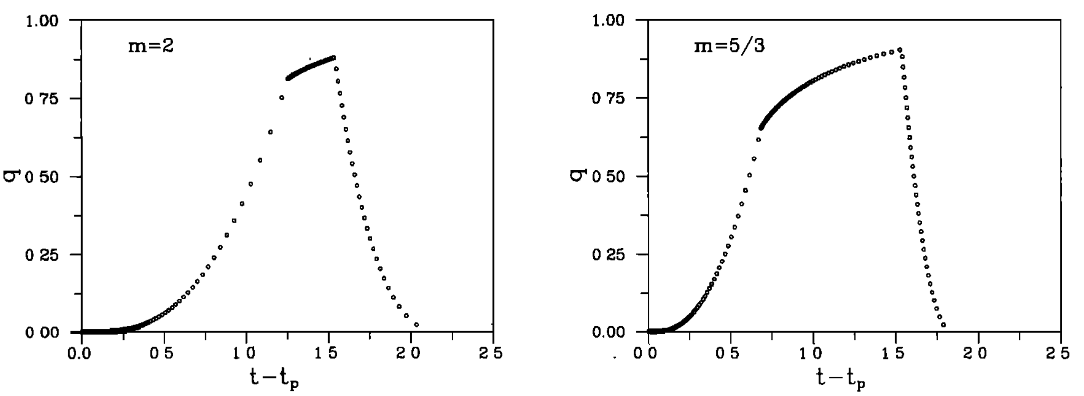

Figure 2. Runoff hydrographs for case A, computed by (a) the analytical solution, $m = 2$ and (b) the semianalytical solution, $m = 5/3$. Time is normalized as in Figure 1, and flow rate is normalized with respect to the ultimate water excess and the plane length, $(r - K_s)L$.

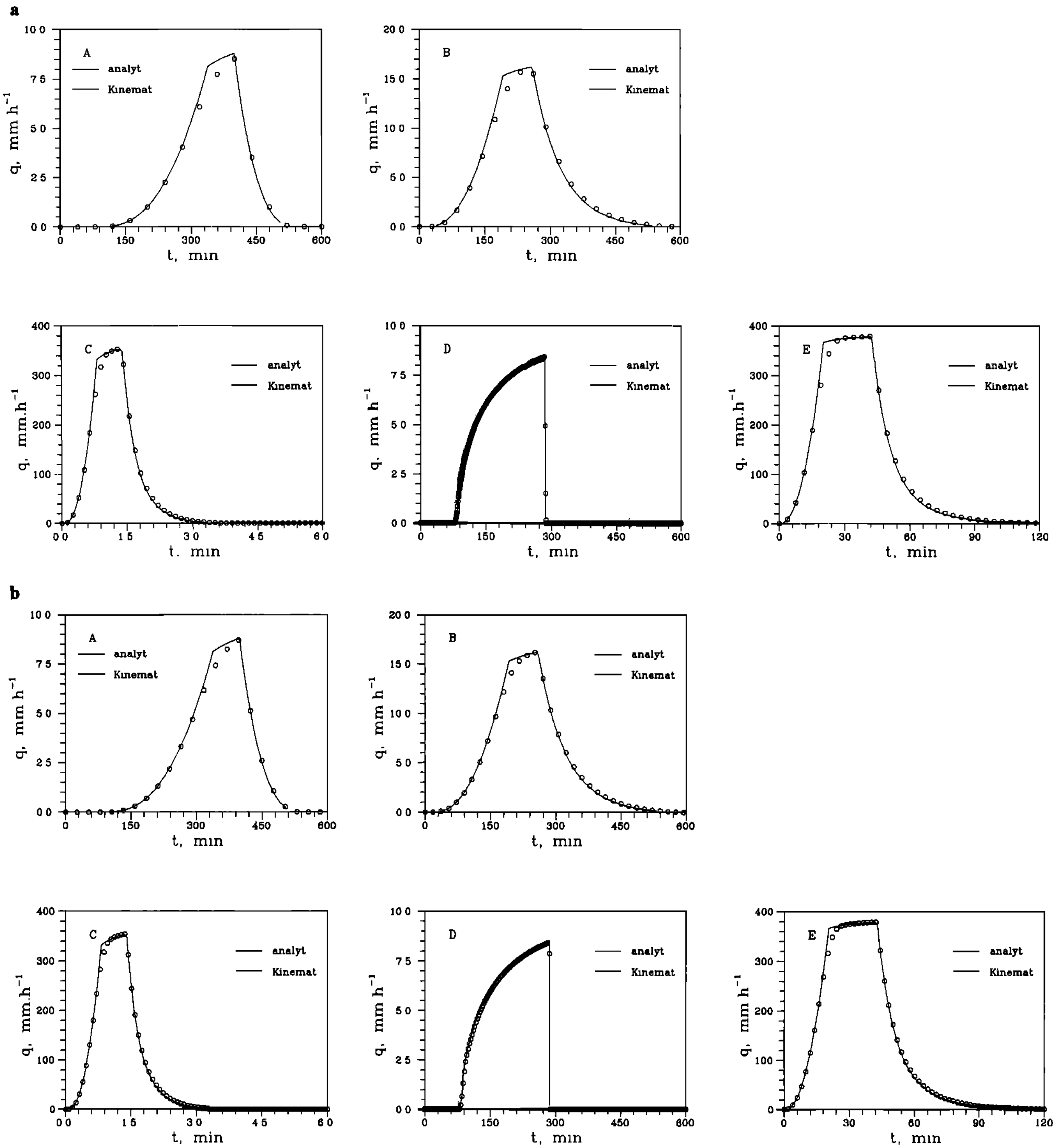

Figure 3. Comparison of runoff hydrographs computed by the analytical solutions and through numerical methods via Kinemat, a simplified version of the KINEROS model, for five different cases of soil, surface, and rainfall conditions: (a) computational time increment as recommended by *Woolhiser et al.*, [1990] and (b) computational time increment, $t_r/10$. Capital letters refer to the cases of Table 1.

gration of the kinematic equations of case A are shown in Figure 1. In Figure 1, corresponding to a process with a high infiltration rate, a slow response time, and a long rainfall duration, a comparison has been made among the analytical solution for the value of the exponent $m = 2$ and the semi-analytical solution where (12), (16), and (22) have been solved numerically using a Gaussian integration. The shapes of the curves are similar before and after the cessation of rainfall, differing only in the exponent m that causes a delay in the characteristic arrival time at the outlet of the plane. The variables in Figure 1 are normalized using

$$x_{\mathrm{NOR}} = L$$
$$t_{\mathrm{NOR}} = S^2/2/K_s^2 \qquad (24)$$

as derived from the infiltration equation (8).

The resulting hydrographs for case A are shown in Figure 2. The hydrograph shapes are similar as should be expected from an examination of the characteristics in Figure 1. Flow rate in the figure is normalized with the normalizing rate,

$$q_{\mathrm{NOR}} = (r - K_s)L \tag{25}$$

Although analytical solutions are possible only for special cases of the exponent in (2) and become cumbersome if rainfall rates change with time, they serve a useful pedagogical purpose and also provide checks on the accuracy of numerical solutions. They can also provide accurate solutions that can be used to develop empirical criteria for selecting maximum time and space increments for numerical solutions. The FORTRAN program, KINEROS [*Woolhiser et al.*, 1990], was modified so the exponent $m = 2$ and hydrographs were calculated numerically for the cases in Table 1. The x increment was $L/15$ as specified in the manual, and the time increments were chosen using the criterion in the KINEROS manual [*Woolhiser et al.*, 1990, p. 101]. This is an ad hoc criterion that establishes five time increments in the rising hydrograph with a net lateral inflow of $r - K_s$. The computational time increments calculated in minutes were 40, 29, 0.13, 0.84, and 3.81 for cases A–E, respectively. Because each of these time increments are equal in dimensionless time (based on the kinematic time to equilibrium at an excess rate of $r - K_s$), they should result in the same level of numerical accuracy if the rainfall excess rate is constant at $r - K_s$. However, they do not take the temporal variability of infiltration rate into account. Comparisons of analytical and numerical hydrographs are shown in Figure 3a and indicate that the criterion for the computational time increments leads to rather good accuracy for cases C, D, and E, but that runoff peaks are underestimated for cases A and B. An alternative approach would be to use the difference between the time of arrival at the downstream boundary of the characteristic originating at $(0, t_p)$ and the time of ponding as an important response time. This time, which we shall call t_t, includes both hydraulic routing and infiltration effects and is the difference between the time of inflection and t_p on the analytical solutions of Figure 3a. Because t_t is always greater than the time to equilibrium at a rainfall excess rate of $r - K_s$, the computational time increment should be shorter than $t_i/5$ if we wish to improve the numerical accuracy of the finite difference scheme used in KINEROS.

Hydrographs computed numerically using a time increment of $t_i/10$ are shown in Figure 3b. The numerical accuracy is acceptable for all cases. This criterion leads to a smaller computational increment for all cases except case D. Case D represents a very short, smooth, steep plane with a low rate of rainfall excess. However, the hydrograph exhibits a rather slow response. Physically, this case is similar to an infiltrometer, with the runoff hydrograph nearly equal to the difference between the rainfall rate and the infiltration rate.

This brief analysis shows that the numerical algorithm in KINEROS provides accurate solutions provided that the appropriate computational time increments are used. It also suggests that the criterion for choice of the time increment in the KINEROS manual could be improved.

Conclusions

A simple variable change leads to an analytical solution for the kinematic wave equations for runoff flow on a plane under constant rainfall for the *Smith and Parlange* [1978] infiltration model. Being restricted to some special cases, the usefulness of the analytical solution is the insight of the problem prior to the application of time-consuming numerical methods.

Acknowledgments. Much of this work was done when the second author was a visiting professor at the Universidad de Córdoba, Spain, on a grant from the Spanish Ministry of Education and Science. This support is gratefully acknowledged. This work has been supported by the Spanish CICYT.

References

Courant, R., and D. Hilbert, *Methods of Mathematical Physics*, vol. 2, Wiley-Interscience, New York, 1962.

Cundy, T. W., and S. W. Tento, Solution to the kinematic wave approach to overland flow routing with rainfall excess given by Philip's equation, *Water Resour. Res.*, *21*, 1132–1140, 1985.

Henderson, F. M., and R. A. Wooding, Overland flow from a steady rainfall of finite duration, *J. Geophys. Res.*, *69*, 1531–1540, 1964.

Hjelmfelt, A. T., Influence of infiltration on overland flow, *J. Hydrol.*, *36*, 179–185, 1978.

Luce, C. H., and T. W. Cundy, Modification of the kinematic wave–Philip infiltration overland flow model, *Water Resour. Res.*, *28*, 1179–1186, 1992.

Sherman, B., Kinematic wave models for overland flow, *Q. Appl. Math.*, *36*, 435–444, 1978.

Sherman, B., and V. P. Singh, A distributed converging overland flow model, 2, Effect of infiltration, *Water Resour. Res.*, *12*, 897–901, 1976.

Singh, V. P., *Kinematic Wave Modeling in Water Resources: Surface Water Hydrology*, John Wiley, New York, 1996.

Smith, R. E., and J.-Y. Parlange, A parameter-efficient hydrologic infiltration model, *Water Resour. Res.*, *14*, 533–538, 1978.

Wooding, R. A., A hydraulic model for the catchment-stream problem, 1, Kinematic wave theory, *J. Hydrol.*, *3*, 254–267, 1965.

Woolhiser, D. A., R. E. Smith, and D. C. Goodrich, *KINEROS, A Kinematic Runoff and Erosion Model*, U.S. Dep. of Agric., Agric. Res. Serv., *Rep. ARS-77*, 1990.

J. V. Giráldez, Departmento de Agronomia, Avda. Menendez Pidal, s/n Apartado de Correos, 3.048, Universidad De Cordoba, 14080, Cordoba, Spain.

D. A. Woolhiser, Department of Civil Engineering, Colorado State University, Foothills Campus, Engineering Research Center, Fort Collins, CO 80521.

(Received November 16, 1995; revised June 26, 1996; accepted July 9, 1996.)